IEEE Photonics Journal
An IEEE Photonics Society Publication

Invited Paper

Integrated Optical Resonators: Progress in 2011

Volume 4, Number 2, April 2012

Amir Arbabi
Lynford L. Goddard

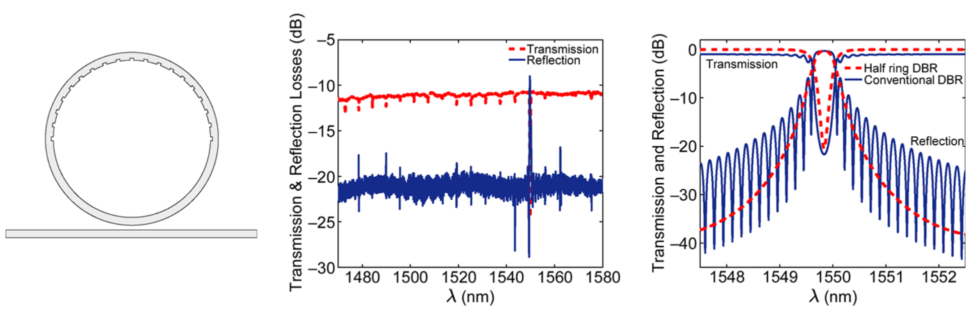

DOI: 10.1109/JPHOT.2012.2189380
1943-0655/$31.00 ©2012 IEEE

Integrated Optical Resonators: Progress in 2011

Amir Arbabi and Lynford L. Goddard

(Invited Paper)

Department of Electrical and Computer Engineering, Micro and Nanotechnology Laboratory,
University of Illinois at Urbana-Champaign, Urbana, IL 61801 USA

DOI: 10.1109/JPHOT.2012.2189380
1943-0655/$31.00 ©2012 IEEE

Manuscript received February 15, 2012; accepted February 24, 2012. Date of current version April 20, 2012. This work was supported by University of Illinois startup funds and National Science Foundation CAREER award ECCS-1055941. Corresponding author: L. L. Goddard (e-mail: lgoddard@illinois.edu).

Abstract: We present a review of the research on integrated optical resonators published in 2011. In particular, we focus on microdisk and microring devices and discuss high-quality factor resonators, methods to tune and trim the resonance wavelength, as well as device applications in optical communications, frequency comb generation, all-optical signal processing, sensing, and single-mode lasers.

Index Terms: Waveguide devices, tunable filters, nanophotonics, four-wave mixing, sensors, integrated nanophotonic systems.

High-quality factor (Q) resonators are useful for a variety of on-chip applications. To achieve high Q, bending and scattering losses must be minimized; therefore, waveguide design and fabrication optimization are necessary. In 2011, Si_3N_4 thin core waveguides were demonstrated with losses as small as 1.1 dB/m at 1310 nm for 5-mm-radius rings (corresponding to intrinsic Q of 2.8×10^7) [1]. Using a thin core and wide waveguide, the sidewall scattering loss, which was the main factor in the total loss, was reduced. Etch-less fabrication techniques were another approach for reducing sidewall roughness. Nezhad *et al.* [2] used patterned hydrogen silsesquioxane (HSQ) ebeam resist as a mask for local oxidation of silicon-on-insulator (SOI) and defined waveguides with 0.35 dB/cm (intrinsic Q of 1.57×10^6) in a 150 μm radius microring resonator (MRR). In another work, Luo *et al.* realized 0.8 dB/cm loss in a 50 μm radius SOI MRR (intrinsic Q of 5.1×10^5) by pattering a thermally grown oxide and using it as a mask to locally oxidize a silicon layer underneath [3].

High Q and large optical intensity enhancement inside integrated resonators comes with high sensitivity of their resonance wavelengths to the geometrical dimensions and fabrication errors. Although high sensitivity is useful for sensing, most other applications require accurate positioning of the resonance wavelengths. Novel methods for trimming and tuning the cavity resonances were introduced and demonstrated in 2011. Real-time trimming and monitoring of resonance wavelengths of GaN/InGaN microdisk cavities by a few nanometers was demonstrated using selective photo-enhanced oxidation. Oxidation happened when a UV laser light illuminated the cavity immersed in deionized water. The water dissolved the oxide, reducing the size of the cavity and blue shifting the resonance wavelengths [4]. Thermal tuning was also used for making adaptive filters. Thermal tuning of the central wavelength of an SOI band pass interference filter by 4 nm, and its full-width at half-maximum (FWHM) by almost a factor of two is reported [5]. The filter was implemented by combining the drop port outputs of two MRRs. Three thermal heaters were used to control the resonance wavelength of the detuned resonators and the relative phase of their drop port outputs. Wavelength referenced temperature tuning with 0.1 pm stability of an integrated resonator was introduced by Zhu *et al.*, which allows for doing spectroscopy in bands where only fixed wavelength nontunable lasers are available [6]. They reported measurement of the transmission spectrum of a whispering gallery microresonator using a fixed probe laser by changing the temperature of the resonator. A tunable pump laser scanning another resonance was used to rapidly change the temperature of the resonator. Sensitivity to environmental temperature was reduced since the resonances at pump and probe wavelength move at almost the same rate. Large tuning of resonance wavelengths of resonators usually involves mechanical movement or resonator shape deformation. Wiederhecker *et al.* used the optical gradient force in a suspended double wheel to tune its resonance by 32 nm with only 13 mW input power [7].

Small footprint, narrow bandwidth, and equidistant resonances of MRRs make them attractive for applications in optical communication and in particular wavelength-division multiplexing (WDM) systems. Integration of 80 SOI MRRs and implementation and characterization of two sets of reconfigurable second-order MRR filter banks for WDM applications were reported in 2011 [8]. Each set of filters contained 20 double MRR filters with 20 GHz bandwidth and 124 GHz spacing. Successful thermal tuning of 11 of the channels was demonstrated, and optical crosstalk smaller than -45 dB between the channels was achieved. Demodulation of non-return-to-zero differential phase-shift keying (NRZ-DPSK) signals using a single MRR was reported previously [9]. Ding *et al.* reported simultaneous demodulation of four WDM channels modulated at 40 Gbits/s using a single SOI MRR with a moderate Q [10]. Two waveguides were coupled to a MRR in the add-drop configuration and alternate-mark inversion (AMI) and duobinary (DB) signals were obtained from the through and drop ports, respectively. Balanced detection by using both AMI and DB signals was shown to improve the receiver sensitivity by about 3 dB, compared with detection using only the AMI signal. Although the demodulation of different channels is done in a single MRR, a wavelength demultiplexer is still required for separation of different channels.

Frequency comb generation has been one of the most successful applications of integrated microresonators in nonlinear optics. Small device size and very high repetition rate make integrated resonators attractive for this application. Generation of a broadband optical frequency comb in a single Si_3N_4 MRR functioning as an optical parametric oscillator (OPO) was demonstrated by Foster *et al.* [11]. The OPO uses the optical Kerr nonlinearity of Si_3N_4 and a cascaded four-wave mixing nonlinear process. With careful design of the waveguide core dimensions, proper anomalous group velocity dispersion was achieved, and a single continuous wave pump laser coupled to the resonator generated a broadband frequency comb spanning a 75 THz bandwidth. The equidistance of the generated comb frequencies over a bandwidth of 14.5 THz was verified using a novel method that was introduced in [11]. Investigation of the coherence of optical frequency combs generated in Si_3N_4 resonators was also reported [12]. A single wavelength pump laser was coupled with MRRs with loaded Q as high as 3×10^6, and the temporal coherence of the output frequency combs were studied. Relative phases of different frequency lines of a comb were adjusted using a programmable pulse shaper for achieving pulse compression. Autocorrelation of the output of the pulse shaper was measured and two different types of frequency combs with different coherence properties were identified. In one type, the generated side bands are one free spectral range (FSR) apart, and their amplitudes drop as their frequency difference with the pump wavelength increases. Such a frequency comb was found to have a high coherence and stable relative phases among different frequency lines. Another type of frequency comb was also identified with primary sidebands separated by a multiple of the FSR and secondary lines with smaller amplitudes and separated by one FSR filling the gap between the primary sidebands. Partial coherence was observed in this type of frequency comb. The physical process responsible for the existence and coherence properties of the two types of frequency combs is not yet known.

Novel applications of MRRs in all-optical signal processing were also reported in 2011. Using reduced Q MRRs (6.5×10^4), first and second-order temporal waveform integrators with temporal resolution of 1.9 ps were realized [13]. First-order integration was made possible due to the

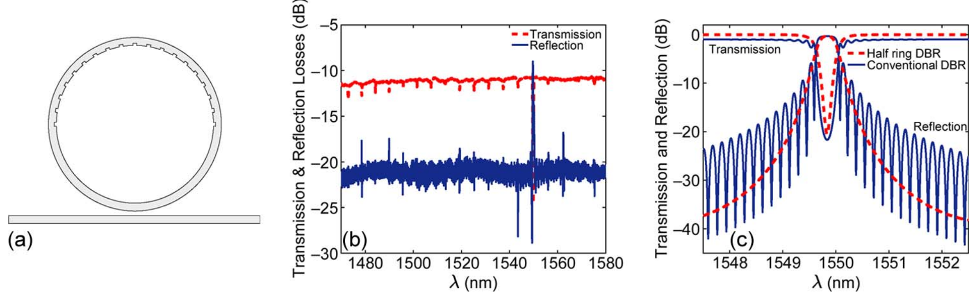

Fig. 1. (a) Schematic of a single wavelength reflector (half ring DBR). Modulation of the waveguide width on the top half of the ring forms a DBR that has its reflection nulls at all ring resonances, except for the one selected for reflection. (b) Measured transmission and reflection spectra of a half-ring DBR fabricated with Si_3N_4 core and SiO_2 cladding. (c) Extracted reflection and transmission spectra of the same device close to its reflection peak. Similar spectra for a 4.3-mm-long conventional DBR with the same reflectivity maximum and FWHM are also shown for comparison. Reprinted with permission from [21]. Copyright 2011, American Institute of Physics.

similarity of a part of the Lorentzian response of the MRR and the transfer function response of a first-order integrator. Second-order integration was achieved by passing the light twice through the same MRR. It was also shown that reduction of Q increases the temporal resolution of the integrators but reduces the integration window.

High Q MRRs have sharp resonance spectra. The center wavelength can be made sensitive to various environmental parameters and thus can be used as the readout for many different types of sensors. In 2011, research efforts vastly expanded the application space of MRRs for sensing as well as focused on improving parameters such as sensitivity and cost. Here, we discuss the results of a few sensor types: refractive index, biological, and acoustic. Scholten *et al.* fabricated high aspect ratio (85 μm tall by 2 μm wide) hollow SiO_x cylinders $(Q > 10^4)$ to form a microfluidic channel sensor where the fluid flows perpendicular to the wafer surface [14]. Hu and Dai used the Vernier effect in cascaded SOI MRRs and suspended the sensing ring to enhance the sensitivity to 4.6×10^5 nm/RIU and achieve a minimum detection limit of 4.8×10^{-6} [15]. For biosensing, Santiago-Cordoba *et al.* reported enhanced sensitivity for protein detection by coupling the evanescent field of a whispering gallery mode resonator to a layer of gold nanoparticles [16], while McClellan *et al.* showed how the health of a soybean leaf can be rapidly quantified in the field using silicon MRRs functionalized with antibodies [17]. Ling *et al.* demonstrated low-noise ultrasound detectors, with a noise equivalent pressure of 21.4 Pa over the 1–75 MHz range, using imprinted polymer MRRs with $Q = 4 \times 10^5$ and a diameter of $D = 60$ μm [18].

Two degenerate counter propagating modes exist at each resonance wavelength of a MRR. These two degenerate modes are uncoupled in an ideal resonator, but a small perturbation can couple them and cause reflection. Engineering this mode coupling for realizing frequency selective reflective devices was theoretically investigated by us [19], and fast numerical simulation and design methods were developed [20]. More recently, we validated these new theoretical models by experimentally realizing a small footprint (30 μm radius) single wavelength reflector with peak power reflectivity of 92.3% and greater than 7.8 dB suppression at adjacent ring resonances across a 100-nm measurement window [21]. A device schematic is shown in Fig. 1(a). Selective coupling of counter propagating modes, i.e., at the 1549.9 nm resonance only, was achieved by patterning a distributed Bragg reflector (DBR) on the inner wall of the MRR's top half. Measured transmission and reflection spectra of the device are shown in Fig. 1(b). The zoomed in view of the extracted spectra of the same device close to its reflectivity peak in Fig. 1(c) shows faster roll-off and no side modes compared with a 4.3 mm conventional linear DBR. This reflective MRR device can be used as a laser mirror for narrow linewidth single-mode semiconductor lasers.

In summary, we highlighted some of the research in 2011 into improving design, fabrication, and performance and the emerging applications of integrated optical resonators.

References

[1] M. Tien, J. F. Bauters, M. J. R. Heck, D. T. Spencer, D. J. Blumenthal, and J. E. Bowers, "Ultra-high quality factor planar Si_3N_4 ring resonators on Si substrates," *Opt. Exp.*, vol. 19, no. 20, pp. 13551–13556, Jul. 2011. [Online]. Available: http://www.opticsexpress.org/abstract.cfm?URI=oe-19-14-13551

[2] M.P. Nezhad, O. Bondarenko, M. Khajavikhan, A. Simic, and Y. Fainman, "Etch-free low loss silicon waveguides using hydrogen silsesquioxane oxidation masks," *Opt. Exp.*, vol. 19, no. 20, pp. 18827–18832, Sep. 2011. [Online]. Available: http://www.opticsexpress.org/abstract.cfm?URI=oe-19-20-18827

[3] L. Luo, G. S. Wiederhecker, J. Cardenas, C. Poitras, and M. Lipson, "High quality factor etchless silicon photonic ring resonators," *Appl. Phys. Lett.*, vol. 19, no. 7, pp. 6284–6289, Mar. 2011. [Online]. Available: http://www.opticsexpress.org/abstract.cfm?URI=oe-19-7-6284

[4] I. Aharonovich, N. Niu, F. Rol, K. J. Russell, A. Woolf, H. A. R. El-Ella, M. J. Kappers, R. A. Oliver, and E. L. Hu, "Controlled tuning of whispering gallery modes of GaN/InGaN microdisk cavities," *Appl. Phys. Lett.*, vol. 99, no. 11, pp. 111111-1–111111-3, Sep. 2011. [Online]. Available: http://apl.aip.org/resource/1/applab/v99/i11/p111111_s1

[5] Y. Ding, M. Pu, L. Liu, J. Xu, C. Peucheret, X. Zhang, D. Huang, and H. Ou, "Bandwidth and wavelength-tunable optical bandpass filter based on silicon microring-MZI structure," *Opt. Exp.*, vol. 19, no. 7, pp. 6462–6470, Mar. 2011. [Online]. Available: http://www.opticsexpress.org/abstract.cfm?URI=oe-19-7-6462

[6] J. Zhu, Ş. K. Özdemir, L. He, and L. Yang, "Optothermal spectroscopy of whispering gallery microresonators," *Appl. Phys. Lett.*, vol. 19, no. 17, pp. 171101-1–171101-3, Oct. 2011. [Online]. Available: http://apl.aip.org/resource/1/applab/v99/i17/p171101_s1

[7] G. S. Wiederhecker, S. Manipatruni, S. Lee, and M. Lipson, "Broadband tuning of optomechanical cavities," *Opt. Exp.*, vol. 19, no. 3, pp. 2782–2790, 2011. [Online]. Available: http://www.opticsexpress.org/abstract.cfm?URI=oe-19-3-2782

[8] M. S. Dahlem, C. W. Holzwarth, A. Khilo, F. X. Kärtner, H. I. Smith, and E. P. Ippen, "Reconfigurable multi-channel second-order silicon microring-resonator filterbanks for on-chip WDM systems," *Opt. Exp.*, vol. 19, no. 17, pp. 306–316, Jan. 2011. [Online]. Available: http://www.opticsexpress.org/abstract.cfm?URI=oe-19-1-306

[9] L. Zhang, J. Yang, M. Song, Y. Li, B. Zhang, R. G. Beausoleil, and A. E. Willner, "Microring-based modulation and demodulation of DPSK signal," *Opt. Exp.*, vol. 15, no. 18, pp. 11564–11569, Sep. 2007. [Online]. Available: http://www.opticsexpress.org/abstract.cfm?URI=oe-15-18-11564

[10] Y. Ding, J. Xu, C. Peucheret, M. Pu, L. Liu, J. Seoane, H. Ou, X. Zhang, and D. Huang, "Multi-channel 40 Gb/s NRZ-DPSK demodulation using a single silicon microring resonator," *J. Lightw. Technol.*, vol. 29, no. 5, pp. 677–684, Mar. 2011. [Online]. Available: http://jlt.osa.org/abstract.cfm?URI=jlt-29-5-677

[11] M. A. Foster, J. S. Levy, O. Kuzucu, K. Saha, M. Lipson, and A. L. Gaeta, "Silicon-based monolithic optical frequency comb source," *Opt. Exp.*, vol. 19, no. 15, pp. 14233–14239, Jul. 2011. [Online]. Available: http://www.opticsexpress.org/abstract.cfm?URI=oe-19-15-14233

[12] F. Ferdous, H. Miao, D. E. Leaird, K. Srinivasan, J. Wang, L. Chen, L. T. Varghese, and A. M. Weiner, "Spectral line-by-line pulse shaping of on-chip microresonator frequency combs," *Nat. Photon.*, vol. 5, no. 12, pp. 770–776, Dec. 2011. [Online]. Available: http://dx.doi.org/10.1038/nphoton.2011.255

[13] M. Ferrera, Y. Park, L. Razzari, B. E. Little, S. T. Chu, R. Morandotti, D. J. Moss, and J. Azaña, "All-optical 1st and 2nd order integration on a chip," *Opt. Exp.*, vol. 19, no. 23, pp. 23153–23161, Nov. 2011. [Online]. Available: http://www.opticsexpress.org/abstract.cfm?URI=oe-19-23-23153

[14] K. Scholten, X. Fan, and E. T. Zellers, "Microfabricated optofluidic ring resonator structures," *Appl. Phys. Lett.*, vol. 99, no. 14, pp. 141108-1–141108-3, Oct. 2011. [Online]. Available: http://apl.aip.org/resource/1/applab/v99/i14/p141108_s1

[15] J. Hu and D. Dai, "Cascaded-ring optical sensor with enhanced sensitivity by using suspended Si-Nanowires," *IEEE Photon. Technol. Lett.*, vol. 23, no. 13, pp. 842–844, Jul. 2011. [Online]. Available: http://ieeexplore.ieee.org/xpls/abs_all.jsp?arnumber=5741827&tag=1

[16] M. A. Santiago-Cordoba, S. V. Boriskina, F. Vollmer, and M. C. Demirel, "Nanoparticle-based protein detection by optical shift of a resonant microcavity," *Appl. Phys. Lett.*, vol. 99, no. 7, pp. 073701-1–073701-3, Aug. 2011. [Online]. Available: http://apl.aip.org/resource/1/applab/v99/i7/p073701_s1

[17] M. S. McClellan, L. L. Domier, and R. C. Bailey, "Label-free virus detection using silicon photonic microring resonators," *Biosens. Bioelectron.*, vol. 31, no. 1, pp. 388–392, Jan. 2012. [Online]. Available: http://www.sciencedirect.com/science/article/pii/S0956566311007445

[18] T. Ling, S. Chen, and L. J. Guo, "High-sensitivity and wide-directivity ultrasound detection using high Q polymer microring resonators," *Appl. Phys. Lett.*, vol. 98, no. 20, pp. 204103-1–204103-3, May 2011. [Online]. Available: http://apl.aip.org/resource/1/applab/v98/i20/p204103_s1

[19] Y. M. Kang, A. Arbabi, and L. L. Goddard, "Engineering the spectral reflectance of microring resonators with integrated reflective elements," *Opt. Exp.*, vol. 18, no. 16, pp. 16813–16825, Jul. 2010. [Online]. Available: http://www.opticsexpress.org/abstract.cfm?URI=oe-18-16-16813

[20] A. Arbabi, Y. M. Kang, and L. L. Goddard, "Cylindrical coordinates coupled mode theory," *IEEE J. Quantum Electron.*, vol. 46, no. 12, pp. 1769–1774, Dec. 2010. [Online]. Available: http://ieeexplore.ieee.org/xpls/abs_all.jsp?arnumber=5638355

[21] A. Arbabi, Y. M. Kang, C. Lu, E. Chow, and L. L. Goddard, "Realization of a narrowband single wavelength microring mirror," *Appl. Phys. Lett.*, vol. 99, no. 9, pp. 091105-1–091105-3, Aug. 2011. [Online]. Available: http://apl.aip.org/resource/1/applab/v99/i9/p091105_s1